Nucleic Acids Research, 1996, Vol. 24, No. 21 **4273–4280**

Ferrocene–oligonucleotide conjugates for electrochemical probing of DNA

Toshihiro Ihara*, Yoshiyuki Maruo, Shigeori Takenaka and Makoto Takagi

Department of Chemical Science and Technology, Faculty of Engineering, Kyushu University, Hakozaki, Higashi-ku, Fukuoka 812-81, Japan

Received June 24, 1996; Revised and Accepted September 24, 1996

ABSTRACT

Toward the development of a universal, sensitive and convenient method of DNA (or RNA) detection, electrochemically active oligonucleotides were prepared by covalent linkage of a ferrocenyl group to the 5′-aminohexyl-terminated synthetic oligonucleotides. Using these electrochemically active probes, we have been able to demonstrate the detection of DNA and RNA at femtomole levels by HPLC equipped with an ordinary electrochemical detector (ECD) [Takenaka,S., Uto,Y., Kondo,H., Ihara,T. and Takagi,M. (1994) *Anal. Biochem.*, 218, 436–443]. Thermodynamic and electrochemical studies of the interaction between the probes and the targets are presented here. The thermodynamics obtained revealed that the conjugation stabilizes the triple-helix complexes by 2–3 kcal mol^{-1} (1–2 orders increment in binding constant) at 298 K, which corresponds to the effect of elongation of additional several base triplets. The main cause of this thermodynamic stabilization by the conjugation is likely to be the overall conformational change of whole structure of the conjugate rather than the additional local interaction. The redox potential of the probe was independent of the target structure, which is either single- or double stranded. However, the potential is slightly dependent (with a 10–30 mV negative shift on complexation) on the extra sequence in the target, probably because the individual sequence is capable of contacting or interacting with the ferrocenyl group in a slightly different way from each other. This small potential shift itself, however, does not cause any inconvenience on practical applications in detecting the probes by using ECD. These results lead to the conclusion that the redox-active probes are very useful for the microanalysis of nucleic acids due to the stability of the complexes, high detection sensitivity and wide applicability to the target structures (DNA and RNA; single- and double strands) and the sequences.

INTRODUCTION

Significant progress in molecular biology has resulted in the identification of more disorders than used to be known directly correlate with the gene expression and enabled us to link some diseases to their responsible specific genes. The benefit in medical applications is immeasurable; for example, specific gene detection permits gene therapy (1–3) and diagnosis (4,5), including even prenatal diagnosis, for several hereditary diseases.

The progress of gene diagnosis requires the development of a simple and sensitive methodology of DNA detection. The most commonly used assay takes advantage of hybridization of a probe with the target DNA; the probe DNA has a complementary sequence for the target and a radioactive label such as ^{32}P (6). Although radioactive isotopes (RI) are widely used as labels because of their high detection sensitivity, due to its hazardous nature and short shelf life, several alternative non-radioactive labelling methods (e.g., fluorescence detection conjugated with the signal amplification using enzymatic reaction) have been developed. Most of these methods, however, require the fixation of sample DNAs followed by the hybridization with a probe on a membrane such as nitrocellulose. Both procedures (fixation and hybridization) are time-consuming and tedious because these are solid-solution heterogeneous reactions. Therefore, a novel method that is quick, convenient and does not rely on radioisotopes is eagerly hoped for.

Electrochemical techniques are potentially sensitive and versatile. The catecholamines, dopamine and norepinephrine, essential participants in the neurotransmission process, are routinely analyzed at fmol levels using HPLC equipped with an electrochemical detector (ECD; 7,8). DNA is, however, redox-inactive under ordinary conditions. Several workers have achieved picogram level quantification of DNA after acidic hydrolysis (9,10). As a reagent for non-destructive labelling of DNA for electrochemical detection, we have already presented the novel DNA ligand in which two aminoacridine parts were connected by a viologen unit (11–13). Although it has interesting characters as an electrochemical probe for studying DNA–ligand interactions, its non-specificity in DNA binding and a cathodic potential applied for probe detection have been obstacles to its analytical applications in gene probing. Toward developing of convenient

*To whom correspondence should be addressed at present address: Department of Applied Chemistry and Biochemistry, Faculty of Engineering, Kumamoto University, Kurokami, Kumamoto 860, Japan. Tel: +81 96 342 3052; Fax: +81 96 342 3679; Email: toshi@chem.kumamoto-u.ac.jp

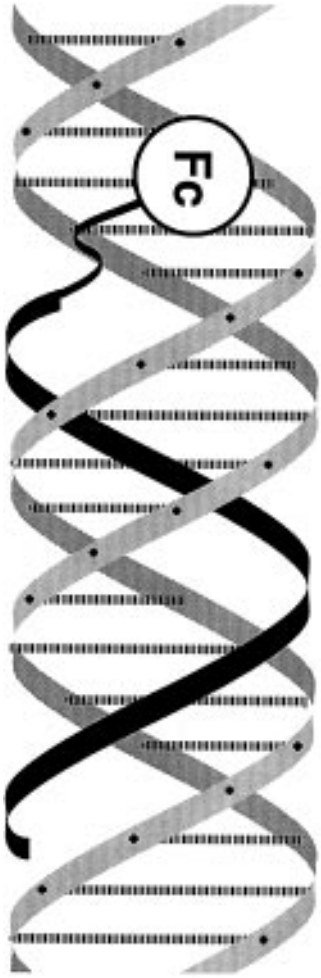

Figure 1. Schematic representation of triple helical local structure including electrochemically active oligonucleotide strand.

method for microanalysis of DNA, ferrocene modified oligonucleotides were synthesized (Fig. 1). These electrochemically active DNA probes should overcome most of the drawbacks and disadvantages of the conventional methods mentioned above. In fact, several demonstrations for this expectation have been presented in our previous work (14).

To establish the basis for the application of ferrocene–oligonucleotide conjugates to practical routine detection of DNA in various phases of gene related study, it is essential to know certain basic characteristics of the ferrocene probe such as binding behavior with complemental ds- or ss-DNA and the related electrochemistry. It is also important to ensure that the ferrocene probe does not introduce any significant, unexpected effects in its interaction with the target DNA. On the other hand, the conjugates could potentially be used as an auxiliary probe for the study of the complexation process of DNA (e.g., double- or triple-stranded structure formation). In this paper, we have studied their thermodynamic and electrochemical properties from the view point as mentioned above.

MATERIALS AND METHODS

Materials

(Dimethylaminomethyl)ferrocene and ferrocenecarboxylic acid were purchased from Aldrich Chemical Co. All dimethoxytrityl nucleoside phosphoramidites, aminolinker phosphoramidite [6-(*N*-trifluoroacetylamino)hexyl-β-cyanoethyl-*N*, *N*-diisopropylphosphoramidite: TFA-Aminolinker Amidite] and support resin for automated DNA synthesis were purchased from Pharmacia Biotech.

Preparation of oligonucleotides

Oligodeoxynucleotides were prepared on a fully automated DNA synthesizer (Pharmacia, Gene Assembler Plus). Synthesized oligodeoxynucleotides are indicated below.

amino-T12:H_2N-$(CH_2)_6$-TTTTT TTTTT TT
***amino-C6T6**:H_2N-$(CH_2)_6$-TT*CCC* T*C*TTT *C*C
T12:TTTTT TTTTT TT
***C6T6**:TT*CCC* T*C*TTT *C*C
A12:AAAAA AAAAA AA
A12at:AAAAA AAAAA AATAT AT
atA12:TATAT AAAAA AAAAA AA
T12at:TTTTT TTTTT TTATA TA
A12gc:AAAAA AAAAA AAGCG CG
gcA12:GCGCG AAAAA AAAAA AA
T12gc:TTTTT TTTTT TTCGC GC
WR:CACGG TAAAA AAAAA AAAGT CCAG
WY:CTGGA CTTTT TTTTT TTTAC CGTG
HP:CTCAA GGGAG AAAGG TTTTC CTTTC
TCCCT TGAG

**C* stands for 5-methyl cytosine.

A standard dimethoxytrityl nucleoside phosphoramidite coupling method was used on a 1.3 μmol CPG support column. For **amino-T12** and **amino-C6T6**, aminohexyl-linker unit was introduced by aminolinker phosphoramidite at the final step of standard phosphoramidite coupling procedure. After completion of the solid-phase synthesis, the liberation of the oligonucleotides from the supports and the removal of protecting groups (except for dimethoxytrityl protecting group on the 5′-hydroxyl terminal) were carried out by incubation in aqueous ammonia (1 ml) in a sealed tube for 12 h at 50°C. The aqueous ammonia was evaporated under reduced pressure at room temperature. From these crude unprotected oligonucleotides, desired oligonucleotides were isolated by two step reversed-phase HPLC (RP-HPLC). LiChrospher 100 RP-18 (e) column (4.6 mm i.d. × 15 cm, Cica-Merck) was used. In the first step, oligonucleotides were purified easily owing to the hydrophobic tag, dimethoxytrityl group on the 5′-end. After detritylation by incubation in 80% acetic acid for 20 min at room temperature, the second step purifications were carried out. HPLC was carried out under the following conditions: temperature, 25°C; flow rate, 1.0 ml min^{-1}; buffer A, 0.1 M triethylammonium acetate (TEAA, pH 7.0); buffer B, acetonitrile; linear gradient, 10–40% B, 10–20% B in 30 min for the first and second step, respectively; detection wavelength, 260 nm. For the purification of pseudo-self-complementary oligonucleotide, **HP**, the crude product was subjected to the electrophoresis on a denatured polyacrylamide gel. The nucleotide was isolated by excising, crushing and elution from the gel. The product was further subjected to GPC (NAP10 Column, Sephadex G-25, Pharmacia Biotech) to remove salts. All isolated oligonucleotides had their

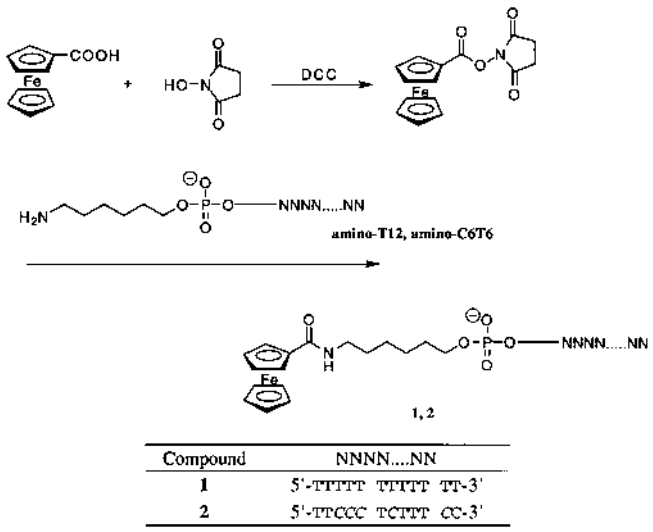

Compound	NNNN....NN
1	5'-TTTTT TTTTT TT-3'
2	5'-TTCCC TCTTT CC-3'

Scheme 1. Synthesis of electrochemically active probes. Italicized C indicates 5-methylcytosine.

homogeneity confirmed by RP-HPLC analysis and after evaporation were stored at –20°C.

The concentration of oligonucleotides were determined by UV absorption at 260 nm, assuming a molar absorptivity coefficient of 15 400, 11 700, 8800, 7300 and 5700 M^{-1} cm^{-1} for A, G, T, C and ^{Me}C, respectively (15), in the denatured state; for **HP**, absorbance measured at 90°C was used.

Preparation of *N*-hydroxysuccinimide ester of ferrocenecarboxylic acid, 3

The synthesis and purification were carried out according to the method previously reported (14).

Preparation of ferrocenyl oligodeoxynucleotides, 1, 2

The synthetic route is illustrated in Scheme 1. The purified aminohexyl-linked oligonucleotides (26 nmol), **amino-T12** and **amino-C6T6**, were dissolved in 20 µl 0.5 M $NaHCO_3/Na_2CO_3$ buffer (pH 9.0). To this was added 6 µl of a dimethylsulfoxide solution of **3** (1.3 µmol) (16). After 10 min sonication of this mixture, in which a yellow precipitate appeared, the suspension was stirred at room temperature overnight. Then, the solution was diluted to 1 ml with TEAA (pH 7.0) and chromatographed on a NAP10 column. The obtained crude material was further purified by RP-HPLC, and the isolated conjugates, **1** and **2**, were stored at –20°C after evaporation.

Hybridization

Hybridization for duplex formation was carried out under appropriate conditions for each duplex according to the empirical equation (17). That for triplex formation was achieved at 5°C for 12 h in a buffer solution used for measurement.

Melting experiments

Absorbance versus temperature curves were measured at 260 nm with a heating and cooling rate of 0.25°C per minute in a Hitachi U-3210 spectrophotometer interfaced with a Hitachi SPR-10 temperature controller. The cuvette-holding chamber was flushed with a constant stream of dry air to avoid water condensation on the cuvette exterior for the duration of the run. Oligonucleotides were dissolved in 20 mM $MgCl_2$, 5 mM NaCl, 1 mM Tris–HCl (pH 7.4).

In general, the melting behavior of triple helical oligonucleotides is biphasic (18–24), which can be described by the two successive equilibria, triplex ⇆ duplex ⇆ coil. In analyzing a duplex–coil transition, a two-state model (25,26) has been used to extract the associated thermodynamic parameters. A similar approach should also be applicable to triplex–duplex transition, since the dissociation of the base pairs in triplex–duplex transition takes place in a highly associated manner as in the duplex–coil transition.

The equilibrium constant for the formation of triplex is now written as

$$K = \frac{\alpha}{(1-\alpha)^2 C} = \exp\left(\frac{-\Delta H^o}{RT} + \frac{\Delta S^o}{R}\right) \qquad [1]$$

where C stands for the concentrations of duplex oligodeoxynucleotide and complementary single-stranded oligonucleotide molecules (the same concentrations in our study). α is the molar fraction of oligonucleotide in the triplex form. ΔH^0 and ΔS^0 are the molar standard enthalpy and standard entropy of triple helix formation, respectively. The absorbance of oligonucleotide is temperature dependent; in general, it indicates linear increase toward temperature rising. This temperature dependence can be corrected by mathematically subtracting the duplex melting curve in the same region. Then, the obtained absorbance change along the temperature axis can be correlated directly with the fraction of triplex, α, i.e., the melting curve can be regarded as a temperature dependence of α value. For obtaining the thermodynamic parameters, the Levenberg–Marquardt non-linear least-squares method was used to fit the corrected melting curve with equation [1]. For fitting equation [1] with the melting curves, we used the curves obtained by heating rate of 0.05°C per minute, in which heating and cooling processes were practically reversible.

Differential titration calorimetry (DTC)

Calorimetric experiments were carried out on an OMEGA titration calorimeter (MicroCal Inc.) for analysis of triplex formation. To exclude the complication related to duplex–coil transition, **HP** was used as a double-stranded target molecule for the formation of triplex, since **HP** forms stable double-stranded hairpin structure because of its entropic advantage of intramolecular base pairing. **HP** in a sample cell was titrated with a concentrated solution of **C6T6** and **2** in a 100 µl stirring syringe rotating at 400 r.p.m. Each oligodeoxynucleotide was dissolved in a buffer solution containing 10 mM $MgCl_2$, 50 mM NaCl and 0.1 M CH_3COOH/CH_3COONa (pH 5.0). A single titration consisted of 15 injections with 5 min intervals. The reference cell of the calorimeter acts as a thermal reference, which was filled with a 0.01% (W/V) aqueous solution of NaN_3. The instrument was calibrated with a standard electrical pulse. Details about this instrument have been described elsewhere (27).

Assuming the duplex–triplex transformation with two-state model, the following equation can be derived (27):

$$\frac{1}{V_0}\left(\frac{dQ}{dC_t}\right) = \Delta H^0\left[\frac{1}{2} + \frac{1 - (1 + r)/2 - C_r/2}{\{C_r^2 - 2C_r(1 - r) + (1 + r)^2\}^{1/2}}\right] \quad [2]$$

where C_t is the total titrant concentration in the sample cell of the volume V_0, Q is the integrated heat absorbed or evolved, and ΔH^0 is the molar heat of binding. C_r and r are defined as C_t/C_d and $1/C_d \cdot K$, where C_d is a duplex, **HP**, concentration that is constant during each titration. The heat of dilution during the titration process was corrected by conducting control experiments. The apparent binding constant, K, and the enthalpy change, ΔH^0, were obtained by optimizing the reproduction of experimental data with equation [2] using nonlinear least-squares program.

Cyclic voltammetry

Electrochemical behavior of the synthesized redox-active probe, **1**, was studied by cyclic voltammetry using a BAS CV-50W voltammetry analyzer with a conventional design of a three-electrodes system. The water jacket of the cell was maintained at 5°C throughout the measurement. A Pt disk (I. D. 1.6 mm), a Pt plate and a standard Ag/AgCl (saturated KCl) electrode were used as working, counter and reference electrode, respectively. Probe **1** and its complementary single- (**A12**, **A12at**, **A12gc**) and double- (**A12-T12**, **atA12-T12at**, **gcA12-T12gc**) stranded oligonucleotides were dissolved (0.5 mM on a strand basis) in 100 µl buffer solution containing 50 mM $MgCl_2$, 50 mM NaCl, and 50 mM Tris–HCl (pH 8.0). The half potentials, $E_{1/2}$, of probe under various solution conditions were obtained using 1st derivation curve of each voltammogram.

RESULTS AND DISCUSSION

Synthesis

The synthesis of electrochemically active oligodeoxynucleic acids (**1** and **2**) is shown in Scheme 1. At the final step of the synthesis, the coupling reaction of the terminal amine of the oligonucleotide and the activated ester of ferrocene carboxylate, **3**, was carried out in an aqueous solution containing 25% dimethylsulfoxide; the solvent composition was optimized with respect to the solubility of both the reactants (**3** still remained undissolved) and the effect of reactivity depression of **3** in aqueous media. The yield for this reaction was relatively high, ~70%, although it was carried out under heterogeneous conditions.

Thermodynamics of probe binding

Melting behaviours of oligonucleotide complexes containing redox-active probe **1** are indicated in Figure 2. The process was monitored by the change in optical absorbance on raising the temperature. The solid curve indicates the melting of the double-stranded complex (**WR–WY**). A definite transition is observed around 60–68°C, which, obviously, corresponds to duplex-to-coil transition. On the other hand, the melting profiles of the three components mixtures (**T12–WR–WY**, **1–WR–WY**), shown by the dotted and the dashed curves, indicate clear biphasic transitions. The transitions at higher temperature are identical to that observed for the duplex melting. Further, a similar biphasic melting curve was obtained in a separate experiment in which **1**, **WR** and **WY** respectively were mixed in a 1:1:1.15 molar ratio. This observation ruled out the possibility that a double-stranded

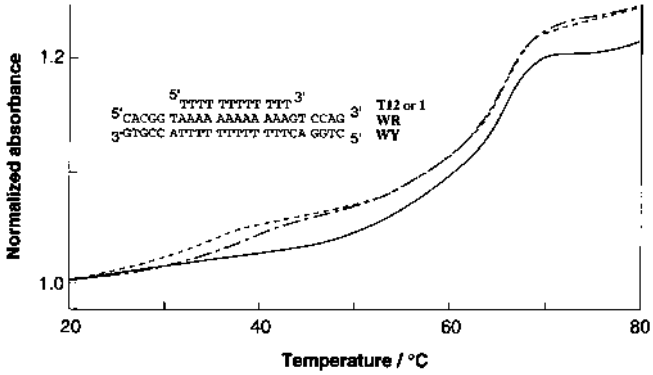

Figure 2. Absorbance at 260 nm versus temperature profiles for the equimolar mixture, **WR–WY** (—), **T12–WR–WY** (- - - -), and **1–WR–WY** (— - —). Measurements were performed in 20 mmol dm^{-3} $MgCl_2$, 5 mmol dm^{-3} NaCl, 1 mmol dm^{-3} Tris–HCl (pH 7.4). Oligonucleotide concentration was 0.5 µmol strand dm^{-3} for all strands. The temperature was increased at a rate of 0.25°C per min.

helix was formed between **1** and **WR** (via Watson–Crick base pairing) to an appreciable extent under the conditions of Figure 3 (data not shown). So, the transitions at lower temperature would correspond to the dissociation of the third strand from the duplex.

Table 1. Biphasic transition of oligonucleotide complexes. Melting points in the high-temperature (T_{mH}) and low-temperature region (T_{mL})(°C)[a]

	Denaturation process		Renaturation process	
	T_{mL}	T_{mH}	T_{mL}	T_{mH}
WY–WR	–	65.8	–	65.0
WY–WR–T12	35.9	65.4	33.9	64.1
WY–WR–1	38.5	66.5	36.4	65.0

[a]0.5 µM oligonucleotide, 20 mM $MgCl_2$, 5 mM NaCl, 1 mM Tris–HCl (pH 7.4); scan rate, 0.25°C/min.

WY: 5′-CTGGACTTTTTTTTTTTTACCGT
WR: 3′-GACCTGAAAAAAAAAAAATGGCA
T12: 3′-TTTTTTTTTTTT
1: 3′-TTTTTTTTTTTT-ferrocenyl

From these experiments, the melting temperatures of the oligonucleotide complexes on the denaturation and renaturation process were calculated and are summarized in Table 1. The larger differences between the transition temperatures on the temperature-raising and the temperature-lowering processes were observed in the transition at lower temperature (T_{mL}). The observation of these hysteresis effects supports the assignments of each transition, because lower reproducibility in the melting curve implies a kinetically slower process, i.e., triplex-to-duplex transition (28).

One should notice that the temperature of the triplex-to-duplex transition is higher for the modified oligopyrimidine than for the unmodified one. This indicates that the modification of oligopyrimidine by ferrocenyl group stabilizes the triple-helix to some extent. It may be due to either one of the following two factors or to some synergistic effect comprising these two factors: (i) the local event around the modified moiety such as the additional

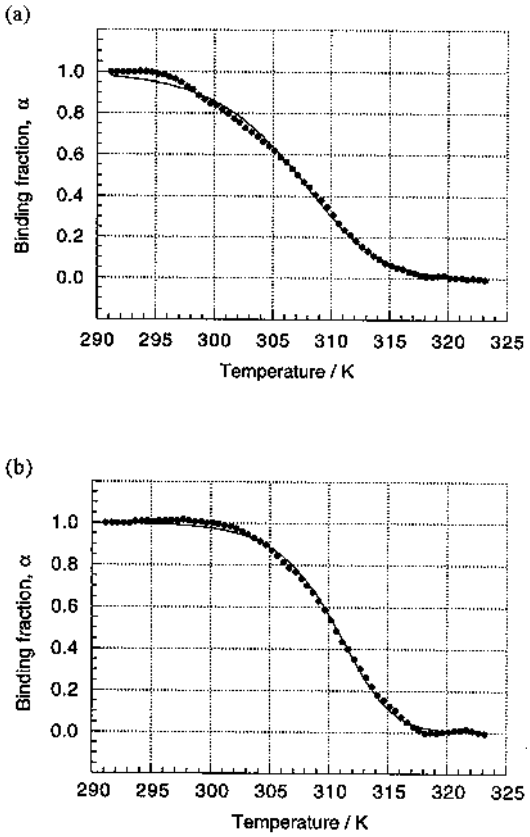

Figure 3. Binding fraction versus temperature for (**a**) **T12–WR–WY** and (**b**) **1–WR–WY**. Closed circles and curves indicate the experimental data and theoretical calculations based on eq. [1], respectively. Experimental data were extracted from the melting experiment that performed by heating rate of 0.05°C per min and absorbance of those were transformed to binding fractions, α, after mathematically subtracting **WR–WY** curve for correction.

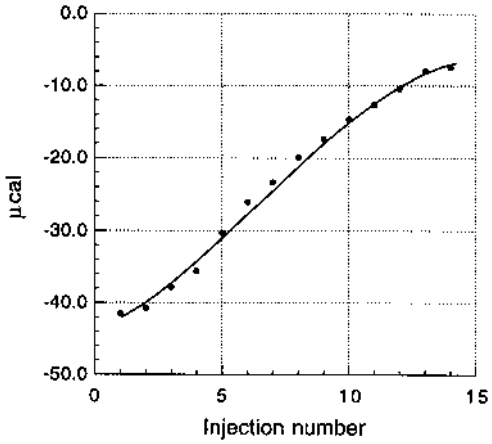

Figure 4. Experimental data and calculated curve (eq. [2]) of calorimetric titration of **2–HP**. Seven μdm^{-3} of 52.5 μmol dm^{-3} **2** was added successively to 1.4 mdm^{-3} of 2.5 μmol dm^{-3} **HP** at 35°C. Both solutions contained 0.1 mol dm^{-3} CH_3COOH/CH_3COONa (pH 5.0), 50 mmol dm^{-3} NaCl, and 10 mmol dm^{-3} $MgCl_2$.

hydrogen bond and the hydrophobic interaction between the modified moiety and the pile of base-pairs in the major groove of double-stranded DNA, and the concurrent conformational change and the desolvation of the ferrocenyl-alkyl group on the triplex formation, (ii) the overall conformational change including the whole oligonucleotide moiety, which is induced by the conjugation with the ferrocenyl-alkyl hydrophobic group. The melting curves in the region of triplex-to-duplex transition and the theoretical curves based on equation [1] are indicated in Figure 3. Both curves show excellent correlation with the corresponding theoretical curves ($r > 0.99$).

The study of triplex formation of the **C6T6** series using melting experiments, like those mentioned above, failed to indicate a clear biphasic behaviour; the resolution between the transition of triplex to duplex and that of duplex to coil was difficult in spite of the extreme stability of intramolecular duplex formed from **HP**. Therefore, DTC was carried out to obtain the thermodynamic parameters of triplex formation of **HP**, with **C6T6** and **2**. The heat generated on addition of **2** to **HP** and the theoretically simulated curve based on equation [2] are shown in Figure 4. The enthalpy changes obtained are relatively large as those observed for triple helix formation. However, the values are within acceptable magnitudes, because triple helix formation and the associated thermodynamic parameters are highly dependent on the sequence, nature and concentration of cations and buffers involved, and, in case of the third strands containing cytosines, on pH (29–31).

The thermodynamic parameters obtained by DTC and melting curve analysis are summarized in Table 2. The enthalpy changes for **C6T6** and **2**, of course, contain that caused by cytosine protonations. Assuming that four protonations accompany the triple helix formation, i.e., two out of six cytosine residues in **C6T6** and **2** are already protonated in their single-strand conformation at pH 5.0 (32), the enthalpy change resulting from these protonations is estimated to be –14.0 kcal mol^{-1} out of the total enthalpy changes. The estimation is based on the enthalpy change of ca. –3.5 kcal mol^{-1} per one protonation that was determined using van't Hoff plot (data not shown), in which the temperature dependence of pK_a (the plot of pK_a versus 1/T) for 5-methyl cytidine was adopted; the pK_a of 4.67, 4.59 and 4.49 were respectively obtained at 293, 304 and 314 K by spectroscopic pH titration.

Anyway, ferrocene conjugation produced enormous enthalpic gain, whereas most (~96% at 298 K) of that was cancelled by its large entropic penalty. On the whole, the overall free energy gain was 2–3 kcal mol^{-1} which corresponds to the increase of binding constants by one or two orders at 298 K. This thermodynamic behaviour is in effect analogous to the introduction of complementary pairing of an additional 4–6 base triplets, which is also the case on the effect of conjugation in the formation of double-stranded complex as reported so far (33). In fact, the enthalpy–entropy compensation was observed in other duplex–triplex transformations including the data for several unmodified-oligonucleotide triplexes reported elsewhere (20,22,23,31,32,34); the plots of $T\Delta S$ against ΔH indicated excellent linearity, $r = 0.993$, as shown in Figure 5. This indicates the similarity between the ferrocene modified- and unmodified-oligonucleotide in their mechanisms of the triplex-forming interactions [however, there is a room for argument about the validity of this relationship (35)].

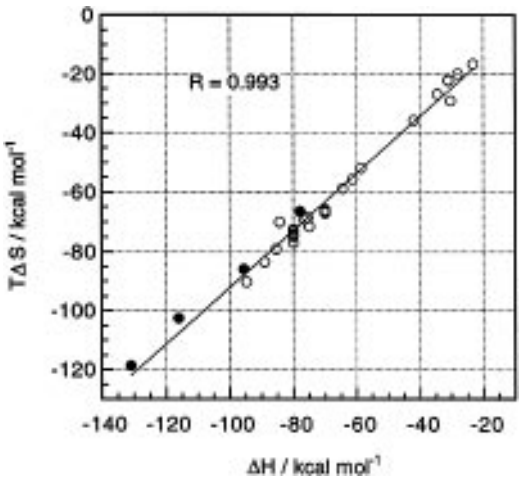

Figure 5. ΔH–ΔS compensation relationship in triple helix formation at 298 K. The data in Table 2 are indicated by filled circles. Open circles indicate the data obtained elsewhere (refs 20,22,23,37,38).

Table 2. Thermodynamic parameters of triple helix formation at 298 K[a]. Ferrocene modified (**1**, **2**) and unmodified (**T12**, **C6T6**) oligopyrimidines

	T12	**1**	**C6T6**	**2**
ΔH/kcal mol^{-1}	77.9	116	95.5	131
ΔS/cal mol^{-1} K^{-1}	223	344	288	398
ΔG_{298}/kcal mol^{-1}	11.4	13.5	9.68	12.4

[a]The parameters were estimated by melting curve fitting with theoretical equation [1] (**T12**, **1**), and DTC measurement using equation [2] (**C6T6**, **2**). It is not meant to compare the parameters between **T12** (or **1**) and **C6T6** (or **2**) directly, because the experimental conditions and the methods used are totally different from each other.

The thermodynamic data presented above strongly suggest that the nature of the driving force stabilizing the triple helix is essentially the same irrespective of the nature of the third strand, i.e., whether the third strand is conjugated with ferrocenyl group or not. This is obviously reflected in the enthalpic gains and entropic penalties imposed by the ferrocene conjugation which are equivalent in magnitude to the introduction of four to six additional base triplets. This magnitude is too large to be solely ascribed to a simple local interaction of a single ferrocene-carbonylamino-alkyl group with the major groove of double-stranded DNA through such processes as additional hydrogen bonding and hydrophobic bonding. The main cause of thermodynamic stabilization of the triple helix by the ferrocene conjugation is, therefore, likely to be the overall conformational change of the whole structure of the single-stranded conjugate oligonucleotide. That is, the conformation of the single-stranded conjugate oligonucleotide in solution is far different, due to the presence of ferrocenyl modification group, from that of the corresponding unconjugated one in solution. However, this never means the lack of the local interaction by the modified group in the major groove of the double-stranded DNA.

The large negative entropy changes for these probes are themselves unfavorable for stabilization of complexes. On the other hand, the negative increment of entropy changes mean the enhancement of cooperativity in triple helix formation as well. The latter feature is quite desirable if we want to use the ferrocene conjugate to reversibly label the target DNA in homogeneous solution. A strong cooperativity in triple helix formation enables us to control the binding of the probe strand to the target simply by adjusting the solution temperature. For example, 90–100% control of the binding ratio is attainable with ease by altering the temperature by only 9 K for probe **2**. This feature means the possibility for recovery of probe and double-stranded target DNA by on/off switching of labelling. On the other hand, the large negative enthalpy changes enable us to attain a significant enhancement of apparent binding constant with lowering the triplex hybridization temperature. A large enthalpy change is synonymous with the high-dependence of the binding constant on temperature. This advantage is further emphasized below by considering the equilibrium of the labelling reaction under highly diluted conditions. The melting temperature or binding ratio of a probe strand is a function of the DNA strand concentration, and the dissociation of probe strand prefers low DNA concentration (25,26). In other words, if one desires a higher detection sensitivity, a probe with a larger binding constant is required. Therefore, lowering the temperature is a valuable and effective expedient for improving the detection limit. Neglecting the change of heat capacity, i.e., assuming $\Delta Cp = 0$, for instance, a binding constant higher than 10^{14} M^{-1} is acquired at 283 K for probe **2**. This permits the probe to bind to its target quantitatively even in pM-strand level concentrations.

Electrochemical properties of probes

Electrochemical studies of the probe were performed by cyclic voltammetry. The voltammograms of (dimethylaminomethyl)ferrocene (**DMAFc**) and free **1** are shown in Figure 6. The symmetrical peaks ($E_{1/2}$ = 0.43 V versus Ag/AgCl), due to reversible redox reaction corresponding to those of ferrocene, were observed for probe **1**, which should be a good confirmation for the existence of a ferrocene moiety in **1**. The maximum current of **1** is only 40% of that of **DMAFc**. This behaviour is reasonable if one considers the expected small diffusion coefficients of **1**. The increased viscosity of the solution which contains **1** may also be countable (36). These effects do not form an obstacle at all in the practical use of **1** so long as the current drop remains at such a level.

As suggested before, the conformation of the probe molecule, particularly the chemical environment around the ferrocenyl group, in single-, double- and triple-stranded DNA structures can not, as yet, be described in detail. There is a possibility that the pendant ferrocenyl group is capable of making some specific contact or interaction with nucleic bases in the nearby sequence. To obtain such information, a cyclic voltammetric study was made at 278 K where all the DNA complexes remain undissociated. The voltammograms obtained for various complexes of probe **1** are summarized in Figure 7. As single-stranded targets, **A12**, **A12at** and **A12gc** were adopted, which formed double-stranded complexes. As double-stranded targets, **A12–T12**, **atA12–T12at** and **gcA12–T12gc** were used, which formed triple-stranded complexes. It was revealed that the electrochemical properties of **1** scarcely depend on its second order structures, i.e., double- and triple-stranded structures. However, they are dependent, though only slightly, on the neighbouring extra sequences of targeted DNA.

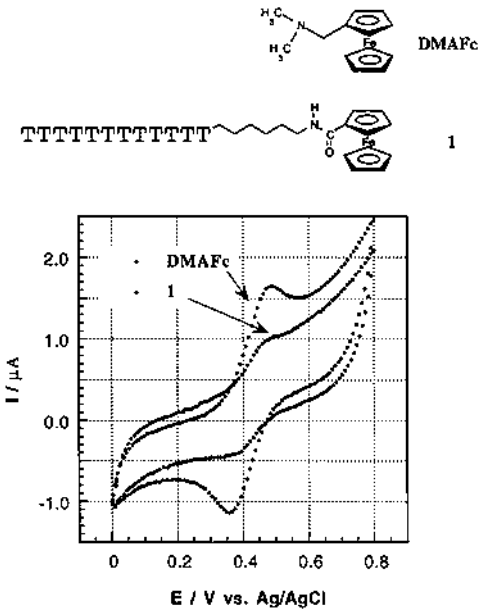

Figure 6. Cyclic voltammograms of 0.5 mmol dm^{-3} **DMAFc** and **1**. Sweep rate, 50 mV sec^{-1}; working electrode, Pt disk; counter electrode, Pt plate; reference electrode, Ag/AgCl. Measurements were carried out in aqueous solution of 50 mmol dm^{-3} $MgCl_2$, 50 mmol dm^{-3} KCl, and 50 mmol dm^{-3} Tris–HCl (pH 8.0) at 5°C. Closed and open circles indicate the voltammograms of **DMAFc** and **1**, respectively.

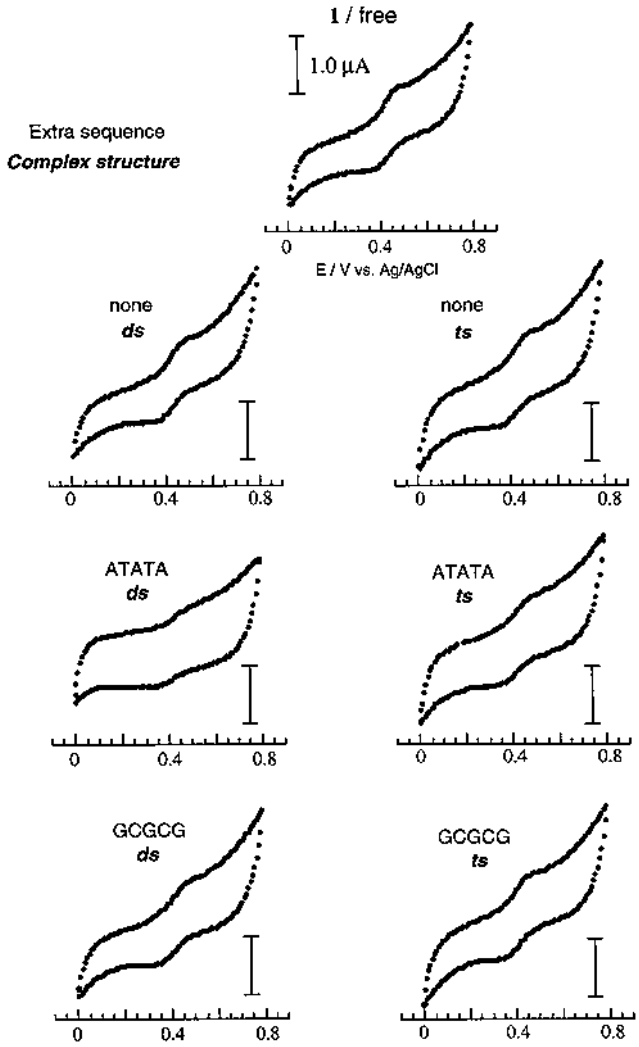

Figure 7. Cyclic voltammograms of 0.5 mmol dm^{-3} **1** in the absence and in the presence of equimolar target oligonucleotide. **A12**, **A12at** and **A12gc** were adopted as single stranded targets. **A12–T12**, **atA12–T12at**, and **gcA12–T12gc** were used as double-stranded targets. The extra sequence and the structure formed with the adopted target are indicated in each voltammogram. Other measurement conditions were the same as that of Figure 6.

The half-wave potentials of **1** complexes are summarized in Table 3. The extra nucleotide rendered the redox potentials of **1** to shift to the negative side, 10–30 mV, while the potentials of the complexes lacking an extra sequence were almost the same as that of free probe **1**. These shifts of redox potentials reflect the change in micro-environment of ferrocene moiety, and provide some information about the structure of the complex (11,36,37). The shift in $E_{1/2}$ can be used to estimate the ratio of binding constants to DNA of **1** and oxidized **1** (**1**$^{\cdot+}$, in which its ferrocene moiety is oxidized to ferrocenium cation). Based on conventional treatment, the ratio of binding constants K_{red}/K_{ox} was calculated to be 0.7–0.3, and, therefore, the **1**$^{\cdot+}$ species is bound to the target DNA ~1.5–3 times more strongly than the **1** species. This reflects the existence of electrostatic interactions between **1**$^{\cdot+}$ and DNA. This means that ferrocene moiety of the probe is favourably located in the complex so as to perform effectively the interaction with the phosphate anions on the DNA backbone when the ferrocenyl group is oxidized to the ferrocenium state. The ferrocenyl group in the probe most probably does not stick out into the bulk solution. In the case of the triple-stranded complex, it is likely that the ferrocenyl moiety lies in the major groove of the double-stranded DNA (Fig. 1), which means the existence of local additional interaction involving the pendant group.

In any event, these small dependencies of redox potential on the target sequence do not cause any inconvenience in the application of the probes for practical DNA detection on HPLC-ECD system. We are now ready to apply this type of probe without any particular consideration for the structure (single- and double helix) and the sequence of the target DNA.

Conclusion

In summary, the ferrocene conjugated oligonucleotides manifested two features: (i) high-dependence of binding constant on temperature and high-cooperative binding, which are associated with a large negative enthalpy and entropy change, respectively, of the complex formation; (ii) insensitivity of their electrochemical response to complex structure (duplex or triplex) and nucleic base sequence; this means that the ferrocenyl probe can serve as a simple and universal electrochemical DNA probe which cannot only simply detect, but also ‘quantify’ the amount of the target DNA sequence in the sample mixture.

The procedure of DNA detection using the present electrochemically active probes comprises two steps: (i) the probe is added into sample solution and the mixture is allowed to reach binding equilibrium at the appropriate temperature and (ii) the mixture is injected into HPLC equipped with an ordinary

Table 3. Cyclic voltammetry half-wave potentials of ferrocenyl oligonucleotide **1** and complexes thereof[a]

NN.....N	Complex structure[b]	$E_{1/2}$ (V, vs. Ag/AgCl)
none	ds	0.434
	ts	0.431
ATATA	ds	0.425
	ts	0.425
GCGCG	ds	0.406
	ts	0.413

[a] Presence of 50 mM $MgCl_2$, 50 mM KCl, 50 mM Tris-HCl (pH 8.0). Pt disk and Pt plate electrodes were used as working and counter electrodes, respectively.
[b] The ds and ts represent double stranded and triple stranded complexes, respectively.

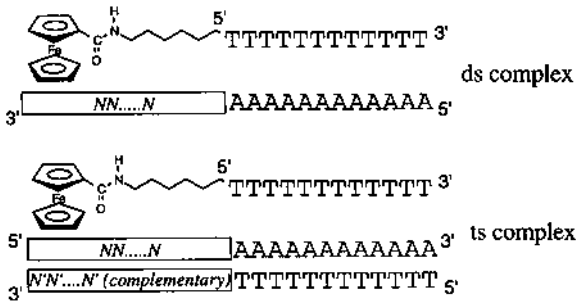

electrochemical detector. Applications were already achieved successfully in the detection of targets such as poly(A), choline transport gene fragment, mRNAs, and oncogene v-*myc* fragment (14). They revealed that the method enabled us to detect a target strand even below femtomole level with ease. This detection limit is comparable with that of radioisotope and that of enzyme linked colorimetric assay (38). These ferrocene-modified oligonucleotides, therefore, have proven to be promising probes for microanalysis of DNA because of their facile procedure for detection, outstanding sensitivity, and invariant response for the target structures and sequences. The methodology proposed here appears to constitute a good candidate for post RI methods. In order to further extend the applicability of this electrochemical method, it is expected that a new electrochemical device will be developed that can read out the loci of the redox-active species on a polyacrylamide gel as 2-D images, as is the case for an ordinary autoradiograph using RI.

ACKNOWLEDGEMENT

This work was partially supported by a Grant-in-Aid for Scientific Research on Priority Areas 'New Development of Organic Electrochemistry' (No. 07215264), and by a Grant-in-Aid for Encouragement of Young Scientists (No. 06750836) from The Ministry of Education, Science and Culture. The authors are also grateful to Research Aid of Watanabe Foundation for Science (T.I.).

REFERENCES

1 Culliton,B.J. (1990) *Science*, **249**, 1372.
2 Rich,D.P., Couture,L.A., Cardoza,L.M., Guiggio,V.M., Armentano,D., Espino,P.C., Hehir,K., Welsh,M. J., Smith,A.E. and Gregory,R.J. (1993) *Hum. Gene Ther.*, **4**, 461–476.
3 Dranoff,G., Jaffee,E., Lazenby,A., Golumbek,P., Levitsky,H., Brose,K., Jackson,V., Hamada,H., Pardoll,D. and Mulligan,R. (1993) *Proc. Natl. Acad. Sci. USA*, **90**, 3539–3543.
4 Murrell,J., Farlow,M., Ghetti,B. and Benson,M.D. (1991) *Science*, **254**, 97–99.
5 Nakano,R., Sato,S., Inuzuka,T., Sakimura,K., Mishina,M., Takahashi,H., Ikuta,F., Honma,Y., Fujii,J., Taniguchi,N. and Tsuji,S. (1994) *Biochem. Biophys. Res. Commun.*, **200**, 695–703.
6 Keller,G.H. and Manak,M.M. (1989) *DNA probes*. Stockton Press, New York.
7 Fenn,R.J., Siggia,S. and Curran,J. (1978) *Anal. Chem.*, **50**, 1067–1073.
8 White,P.C. (1984) *Analyst*, **109**, 677–697.
9 Kafil,J.B., Cheng,H.-Y. and Last,T.A. (1986) *Anal. Chem.*, **58**, 285–289.
10 Nakahara,T., Shiraishi,A., Hirano,M., Matsumoto,T., Kuroki,T., Tatebayashi,Y., Tsutsumi,T., Nishiyama,K., Ooboshi,H., Nakamura,K., Yao,H., Waki,M. and Uchimura,H. (1989) *Anal. Biochem.*, **180**, 38–42.
11 Takenaka,S., Ihara,T. and Takagi,M. (1990) *J. Chem. Soc., Chem. Commun.*, 1485–1487.
12 Takenaka,S., Sato,H., Ihara,T. and Takagi,M. (1991) *Anal. Sci., Suppl.*, **7**, 1385–1386.
13 Takenaka,S., Ihara,T. and Takagi,M. (1992) *Chem. Lett.*, 1–4.
14 Takenaka,S., Uto,Y., Kondo,H., Ihara,T. and Takagi,M. (1994) *Anal. Biochem.*, **218**, 436–443
15 Beal,P.A. and Dervan,P.B. (1992) *J. Am. Chem. Soc.*, **114**, 4976–4982.
16 Applied Biosystems (1989) Model 370 User Bulletin 11.
17 Sambrook,J., Fritsch,E.F. and Maniatis,T. (1989) *Molecular Cloning: A Laboratory Manual*, Cold Spring Harbor Laboratory Press, Cold Spring Habor, NY.
18 Mergny,J.-L., Collier,D., Rougée,M., Montenay-Garestier,T. and Hélène,C. (1991) *Nucleic Acids Res.*, **19**, 1521–1526.
19 Riley,M., Maling,B. and Chamberlin,M.J. (1966) *J. Mol. Biol.*, **20**, 359–389.
20 Pilch,D.S., Brousseau,R. and Shafar,R.H. (1990) *Nucleic Acids Res.*, **18**, 5743–5750.
21 Pilch,D.S., Levenson,C. and Shafer,R.H. (1990) *Proc. Natl. Acad. Sci.USA*, **87**, 1942–1946.
22 Plum,G.E., Park,Y.-W., Singleton,S.F., Dervan,P.B. and Breslauer,K.J. (1990) *Proc. Natl. Acad. Sci.USA*, **87**, 9436–9440.
23 Roberts,R.W. and Crothers,D.M. (1991) *Proc. Natl. Acad. Sci.USA*, **88**, 9397–9401.
24 Mergny,J.-L., Sun,J.-S., Rougée,M., Montenay-Garestier,T., Bercelo,F., Chomilier,J. and Hélène,C. (1991) *Biochemistry*, **30**, 9791–9798.
25 Petersheim,M. and Turner,D.H. (1983) *Biochemistry*, **22**, 256–263.
26 Sugimoto,N., Tanaka,A., Shintani,Y. and Sasaki,M. (1991) *Chem. Lett.*, 9–12.
27 Wiseman,T., Williston,S., Brandts,J.F. and Lin,L.-N. (1989) *Anal. Biochem.*, **179**, 131–137.
28 Rouge,M., Faucon,B., Mergny,J.L., Barcelo,F., Giovannangeli,C., Garestier,T. and Hlne,C. (1992) *Biochemistry*, **31**, 9269–9278.
29 Singleton,S.F. and Dervan,P.B. (1992) *Biochemistry*, **31**, 10995–11003.
30 Singleton,S.F. and Dervan,P.B. (1993) *Biochemistry*, **32**, 13171–13179.
31 Singleton,S.F. and Dervan,P.B. (1994) *J. Am. Chem. Soc.*, **116**, 10376–10382.
32 Manzini,G., Xodo,L.E., Gasparotto,D., Quadrifoglio,F., van der Marel,G.A. and van Boom,J.H. (1990) *J. Mol. Biol.*, **213**, 833–843.
33 Knorre,D.G., Vlassov,V.V., Zarytova,V.F., Lebedev,A.V. and Federova,O.S. (1994) *Design and Targeted Reagents of Oligonucleotide Derivatives*. CRC Press, Boca Raton, FL.
34 Yoon,K., Hobbs,C.A., Walter,A.E. and Turner,H. (1993) *Nucleic Acids Res.*, **21**, 601–606.
35 Krug,R.R., Hunter,W.G. and Grieger,R.A. (1976) *J. Phys. Chem.*, **80**, 2335–2341.
36 Carter,M.T. and Bard,A.J. (1987) *J. Am. Chem. Soc.*, **109**, 7528–7530.
37 Carter,M.T., Rodriguez,M. and Bard,A.J. (1989) *J. Am. Chem. Soc.*, **111**, 8901–8911.
38 Beck,S. and Köster,H. (1990) *Anal. Chem.*, **62**, 2258–2270.